O-GlcNAcylation mediates endometrial cancer progression by regulating the Hippo-YAP pathway

LIANGHAO ZHAI[1*], XIAOSHAN YANG[2,3*], JIAN DONG[1*], LUOMENG QIAN[4], YUNGE GAO[1], YANHONG LV[1], LIGANG CHEN[1], BILIANG CHEN[1] and FUXING ZHOU[1]

[1]Department of Gynecology and Obstetrics, Xijing Hospital, Air Force Medical University, Xi'an, Shaanxi 710032; [2]Stomatology Hospital, Southern Medical University, Guangzhou, Guangdong 510280; [3]State Key Laboratory of Military Stomatology and National Clinical Research Center for Oral Diseases and Shaanxi International Joint Research Center for Oral Diseases, Center for Tissue Engineering, School of Stomatology, Air Force Medical University, Xi'an, Shaanxi 710032; [4]Department of Medicine, Nankai University, Tianjin 300071, P.R. China

Abstract. The incidence of endometrial cancer (EC) is rapidly increasing worldwide. The majority of endometrial cancers are diagnosed at an early stage and are associated with a good prognosis; however, patients with advanced-stage EC have a poor prognosis and present with invasive metastasis. The mechanisms responsible for the invasion and metastasis of endometrial cancer remain unknown. Here, the present study aimed to examine the effects of *O*-GlcNAcylation on the malignancy of EC and its association with Yes-associated protein (YAP). It was found that the expression of *O*-GlcNAc transferase (OGT) and *O*-GlcNAcylation were increased in EC tissues; the decrease in *O*-GlcNAcylation levels was found to lead to the decreased proliferation, migration and invasion of EC cells. Mass spectrometric analysis revealed that OGT knockdown reduced the *O*-GlcNAcylation of YAP. Furthermore, it was found that the reduction in the *O*-GlcNAcylation of YAP promoted its phosphorylation, which in turn inhibited the access of YAP to the nucleus and downstream target gene activation, demonstrating that the level of *O*-GlcNAcylation affects the development of EC. On the whole, the findings of the present study indicate that YAP is a key molecule linking the *O*-GlcNAcylation and Hippo pathways, which together regulate the progression of EC.

Correspondence to: Dr Fuxing Zhou or Dr Biliang Chen, Department of Gynecology and Obstetrics, Xijing Hospital, Air Force Medical University, 127 Changle West Road, Xincheng, Xi'an, Shaanxi 710032, P.R. China
E-mail: zhoufuxing1234@126.com
E-mail: cblxjh@fmmu.edu.cn

*Contributed equally

Introduction

Endometrial cancer (EC), a common, malignant tumor presenting in young individuals, has a high invasiveness and low differentiation, and has become a major threat to the health of women worldwide (1,2). Despite early diagnostic and therapeutic developments in recent years, patients with late-stage EC still have a poor prognosis and exhibit aggressive metastases (3). Hence, in order to determine effective intervention strategies for EC, the exploration of the mechanisms underlying its occurrence and development is critical.

Metabolic disorders, such as diabetes, are a major risk factor for EC progression (4). Hyperglycemia leads to an increase in the activity of the hexosamine biosynthesis pathway to promote *O*-GlcNAcylation, which is a necessary post-translational modification (PTM) (5,6). The entire process is both reversible and dynamic, and is driven by *O*-GlcNAc transferase (OGT) and inverted by *O*-GlcNAcase (OGA) (7). *O*-GlcNAcylation is involved in numerous key cellular behaviors, such as translation, metabolism and apoptosis, with the potential to alter protein function either indirectly or directly in concert with phosphorylation (8,9). The dysregulation of *O*-GlcNAc metabolism has been linked to a variety of diseases, including diabetes, cancer and inflammation (10-12). A wide variety of molecules, closely related to tumorigenesis and cancer development, are modified by *O*-GlcNAcylation, which affects their proliferative, invasive and metabolic properties (13-15). Although aberrant *O*-GlcNAcylation is associated with EC cell invasion and metastasis (16,17), the mechanisms through which *O*-GlcNAcylation influences the development and progression of EC remain unclear.

The Hippo pathway is an evolutionarily conserved tumor suppressor pathway that regulates organ development and maintains internal environment homeostasis (18-20). Yes-associated protein (YAP) is a transcriptional co-activator and a key component of the Hippo pathway (21). Activated macrophage stimulating 1/2 phosphorylates and activates its substrate, large tumor suppressor kinase 1/2 (LATS1/2), when the Hippo pathway is operating, which in turn directly

causes downstream YAP phosphorylation and inactivates it by promoting its cytoplasmic retention. The inhibition of the Hippo pathway causes YAP to enter the nucleus in a non-phosphorylated state and bind to transcription factors, such as the TEA domain protein family, to promote cell proliferation and transformation (22,23). High glucose levels activate YAP signaling (24-26), which is critical to the development of cancers, including EC (27-29). Moreover, YAP is a target protein for *O*-GlcNAc modification (30); however, to date, at least to the best of our knowledge, there are no relevant studies available on EC that depict this mechanism. The present study thus aimed to examine the effects of *O*-GlcNAcylation on the malignancy of EC and its association with YAP.

Materials and methods

Cells and cell culture. The AN3CA (CL-0505) and HEC-1-B (CL-0100) cell lines, provided by Procell Life Science & Technology Co., Ltd., were cultured at 37°C and 5% CO_2 in MEM supplemented with 10% fetal bovine serum (FBS, Gibco; Thermo Fisher Scientific, Inc.). OSMI-1 (HY-119738, MedChemExpress) and Thiamet-G (TMG; HY-12588, MedChemExpress) were dissolved in dimethyl sulfoxide (DMSO; PYG0040, Wuhan Boster Biological Technology, Ltd.).

Generation of stable cell lines. The AN3CA (50,000 cells/well) and HEC-1-B (50,000 cells/well) cells were cultured for 24 h in six-well plates and the medium was discarded. Subsequently, 940 μl medium, 40 μl infection enhancing solution (HitransG P, 25X) and 20 μl virus (1x10⁸ TU/ml) were added to the six-well plates followed by incubation at 37°C for 12 h. After switching to normal medium and continuing incubation for 48 h, the cells were cultured in medium containing puromycin (2 μg/ml, HY-K1057, MedChemExpress) for 2 weeks to establish a stable cell line. The third generation was used. The MOI values of both cell lines were 10. Virus and infection enhancement solution were provided by Shanghai Genechem Co., Ltd. The sequences of the shRNAs used are presented in Table SI.

Western blot analysis. The cells were treated with RIPA lysis buffer (cat. no. AR0102, Wuhan Boster Biological Technology, Ltd.) containing phosphatase inhibitors (cat. no. AR1195, Wuhan Boster Biological Technology, Ltd.) and broad-spectrum protease inhibitors (cat. no. AR1193, Wuhan Boster Biological Technology, Ltd.), and whole protein lysates were harvested. The protein concentration was determined using the BCA protein concentration assay kit (cat. no. P0012S, Beyotime Institute of Biotechnology). Equal amounts of 50 μg whole cell lysate were separated on 10% SDS-PAGE gel and then electrophoretically transferred to PVDF membrane. After being blocked with 10% skimmed milk in TBST at 27°C for 1 h, the PVDF membranes were incubated overnight at 4°C with primary and secondary antibodies, followed by ECL luminescence detection (cat. no. AR1196, Wuhan Boster Biological Technology, Ltd.). Analysis of the strips was performed using ImageJ software (V1.8.0.112, National Institutes of

Health). The antibodies and dilutions used in the present study were as follows: Anti-OGT (1:1,000; cat. no. ab96718, Abcam), anti-*O*-GlcNAcylation (1:1,000; cat. no. ab2739, Abcam), anti-YAP (1:2,000; cat. no. 13584-1-AP, Proteintech Group, Inc.), anti-phosphorylated (p-)YAP (1:1,000; cat. no. 13008S, Cell Signaling Technology, Inc.), anti-LATS1 (1:1,000; cat. no. 3477S, Cell Signaling Technology, Inc.), anti-LATS2 (1:1,000; cat. no. 20276-1-AP, Proteintech Group, Inc.), anti-connective tissue growth factor (CTGF; 1:2,000; cat. no. 25474-1-AP, Proteintech Group, Inc.), anti-Histone-H3 (1:2,000; cat. no. 17168-1-AP, Proteintech Group, Inc.), anti-β-actin (1:2,000; cat. no. BM0005, Wuhan Boster Biological Technology, Ltd.) and anti-tubulin (1:1,000; cat. no. 2148, Cell Signaling Technology, Inc.).

Co-immunoprecipitation. Cell lysates were obtained according to the kit instructions (AM001-01, ACE Biotechnology LLC) and incubated with 20 μl of prepared protein A/G immunoprecipitated magnetic beads (IC-8110, InCellGene LLC) for 12 h at 4°C according to the instructions of the manufacturer. Following magnetic separation, the target antibody was added to the antigen-magnetic beads and incubated at 4°C for 12 h. The antigen was then eluted and the eluted antigen was examined using western blot analysis. The antibodies used for immunoprecipitation were as follows: Anti-OGT (1:200; cat. no. ab96718, Abcam), anti-IgG (1:200; cat. no. IC-8109, InCellGene LLC), anti-*O*-GlcNAcylation (1:200; cat. no. ab2739, Abcam), anti-YAP (1:200; cat. no. 13584-1-AP, Proteintech Group, Inc.), anti-LATS1 (1:200; cat. no. 3477S, Cell Signaling Technology, Inc.) and anti-LATS2 (1:200; cat. no. 20276-1-AP, Proteintech Group, Inc.).

Immunohistochemistry. Human endometrial cancer tissue microarray slides were purchased from Shanghai Xinchao Biotechnology (cat. no. HUteA060CS01). Ethics approval (no. KY20203047) was provided by the Medical Ethics Committee of the First Hospital Affiliated to the Air Force Medical University. The slides included 28 endometrial cancer specimens (age range, 36-73 years) and 15 pairs of carcinomas and para-cancerous tissue specimens (age range, 36-73 years). Dewaxing and rehydration were followed by antigen repair in citrate buffer at pH 6.0. The sections were closed with endogenous peroxidase blocking solution for 10 min, followed by immersion in PBS solution for 5 min. Incubation with primary antibody was performed overnight at 4°C after the sections are closed with goat serum (cat. no. AR0009, Wuhan Boster Biological Technology, Ltd.). The primary antibodies used were as follows: Anti-OGT (1:100; cat. no. PB9767, Wuhan Boster Biological Technology, Ltd.) and anti-*O*-GlcNAc (1:50; cat. no. PTM-952, Jingjie PTM BioLab (Hangzhou) Co. Ltd.). The sections were then incubated with secondary antibodies (1:1; cat. no. BA1056, Wuhan Boster Biological Technology, Ltd.) at 37°C for 1 h following three washes with PBS. Dropwise additions of HRP-streptavidin (cat. no. BA1088, Wuhan Boster Biological Technology, Ltd.) were added, followed by DAB color development. The tissue microarray was scanned using a microscope (Pannoramic MIDI, 3DHISTECH) and the histochemistry score (H-SCORE) was calculated by analyzing

the histochemical results using Aperio ImageScope software (Version 12, Leica Biosystems).

Cell viability assays. The AN3CA and HEC-1-B cells were seeded in 96-well plates (5,000 cells/well for AN3CA cells and 8,000 cells/well for HEC-1-B cells). Measurements were performed at pre-determined time points. Cell Counting Kit-8 (CCK-8; BB-4202, Bestbio) solution was added to the 96-well plates, and following incubation for 2 h with protection from light, spectrophotometric measurements were carried out at 450 nm using an Infinite M200PRO multimode plate reader (Tecan Group, Ltd.).

The cells were seeded in a 96-well plate and incubated at 37˚C for 24 h prior to the addition of 100 μl EdU (50 μM, cat. no. C10310, Guangzhou RiboBio Co., Ltd.). After 2 h, the 96-well plate was washed with PBS, and the cells were fixed with 4% paraformaldehyde at 27˚C for 30 min, and glycine (2 mg/ml, AR1200, Boster Biological Technology, Ltd.) was then added to the cells and incubated at 27˚C for 5 min. After washing with PBS, cells were incubated at 27˚C for 10 min following the adding 0.5% TritonX-100. Subsequently, Apollo staining and DNA staining were performed according to the instructions of the manufacturer (C0085, Beyotime Institute of Biotechnology). Finally, observation was performed using a fluorescence microscope (Nikon Eclipse Ni-U).

Wound healing assay. The cells were inoculated in six-well plates ($1.5x10^6$ cells/well), cultured for 12 h and then serum-starved for 24 h. A 50 μl pipette tip was passed through the cell monolayer to create a 'wound'. To control for the possible effects of proliferation, serum-free medium was used for cell culture. Images of the wound area were obtained in a fixed location once a day using an inverted microscope (Nikon Eclipse Ti2; Nikon Corporation), and wound closure rates were calculated using ImageJ software (V1.8.0.112, National Institutes of Health).

Transwell assay. Transwell assays were employed to evaluate the invasive and migratory potential of the cells. For the detection of the cell invasive ability, 100,000 cells were added to the upper chamber of the Transwell (354480, Matrigel Biocoat Invasion Chambers, Corning, Inc.). For the detection of the migratory ability, 30,000 cells were added to the upper chamber (3422, Corning Transwell, Corning, Inc.). It is important to note that the lower chamber contained 10% FBS, while the upper chamber did not. The upper chamber was removed 48 h following incubation at 37˚C, and the Transwell membrane fixed with 4% paraformaldehyde at 27˚C for 30 min and stained with crystal violet (C0121, Beyotime Institute of Biotechnology) at 27˚C for 5 min. After dissolving the crystal purple dye in 33% acetic acid, the absorbance was measured at 570 nm using TECAN Infinite M200 Pro (Tecan Group, Ltd.).

Mass spectrometric analysis. The cells were treated with RIPA lysis buffer containing phosphatase inhibitors and broad-spectrum protease inhibitors, and whole protein lysates were harvested. The extracted protein was added to dithiothreitol (10 mM, M109-5G, Amresco, LLC). This was followed by incubation at 37˚C for 1 h and iodoacetamide was then added (40 mM, M216-30G, Amresco, LLC) followed by incubation at 37˚C for 45 min. The samples were then diluted using ammonium bicarbonate (A6141, MilliporeSigma) to the pH of the sample of 8. Trypsin (V5280, Promega Biotech Co., Ltd.) was added at a 50:1 ratio of protein to trypsin overnight at 37˚C. The samples were passed through a desalting column and eluted with 70% acetonitrile. The enrichment of the glycosylated peptides was then performed by adding the samples to the activated hydrophilic interaction liquid chromatography enrichment column (Atlantis, Waters) and incubating at 27˚C for 2 h; the flow-through solution was discarded. For one more elution, 0.5% formic acid was added to 5% acetonitrile +0.5% formic acid. The flow-through solution was collected and lyophilized. The samples were analyzed using high-performance liquid chromatography coupled with a Q Exactive HF mass spectrometer (Thermo Fisher Scientific, Inc.). The *Homo sapiens* SP database was searched using Byonic software (Protein Metrics Inc). The search parameters were set as follows: 15 ppm for precursor ion mass tolerance, 0.02 Da for fragment ion mass tolerance, 2 for the maximum number of missed cleavages, and the Dynamic Modification was set to M Oxidation (15.995 Da) and Acetyl (Protein N-terminal).

GeneCards. The GeneCards database (www.genecards.org) provides a comprehensive and authoritative summary of human gene annotation data (31). The GeneCards database was searched using 'endometrial cancer' to obtain genes associated with endometrial cancer.

RNA extraction and reverse transcription-quantitative PCR (RT-qPCR). The RNAsimple Total RNA kit (Tiangen Biotech Co., Ltd.) was used to isolate total RNA from the EC cells, and the PrimerScript RT Reagent kit (Takara Bio, Inc.) was used for reverse transcription. qPCR was performed using ChamQ Universal SYBR qPCR Master Mix (Vazyme Biotech Co., Ltd.) and the CFX Connect system (Bio-Rad Laboratories, Inc.). The PCR thermocycling conditions were set according to the kit instructions (Vazyme Biotech Co., Ltd.). The $2^{-\Delta\Delta Cq}$ method (32) was used to calculate the relative transcript levels of target genes, and ACTIN was used as an internal reference. The genes examined were: ankyrin repeat domain 1 (ANKRD1), connective tissue growth factor (CTGF), cysteine-rich angiogenic inducer 61 (CYR61) and glucose transporter 3 (GLUT3). The primers used for RT-qPCR in the present study are presented in Table SII.

Cycloheximide (CHX) chase experiments. The medium was changed to medium containing 50 μM CHX (HY-12320, MedChemExpress) when the cell density in the culture dish reached 70%. The time of medium change was considered as the beginning of receiving CHX treatment, and different treatment times (0, 4, 8, 12, 16 and 24 h) were selected for protein extraction and western blot analysis.

Immunofluorescence staining. The cells were seeded in confocal Petri dishes one day in advance. At 37˚C, following fixation with 4% paraformaldehyde for 15 min, the cells were
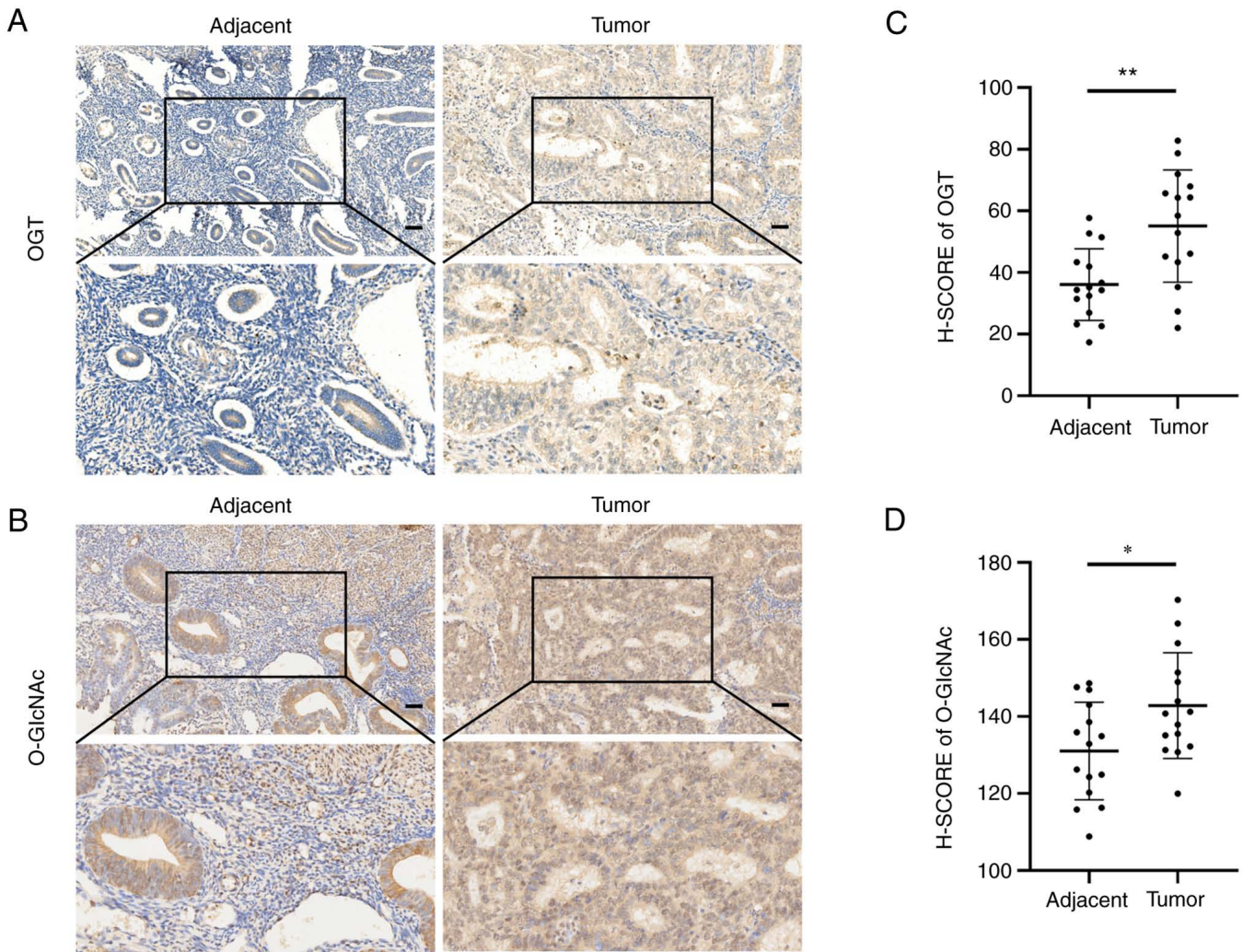
Figure 1. OGT and *O*-GlcNAc expression levels are upregulated in EC tissues. (A and B) Immunohistochemical staining of OGT and *O*-GlcNAc in EC tumor and paired tumor-adjacent tissue sections. Scale bars, 50 μm. (C and D) H-SCORE of OGT and *O*-GlcNAc in cancer tissues and paired tumor-adjacent tissues. *P<0.05 and **P<0.01. OGT, *O*-GlcNAc transferase; EC, endometrial cancer; H-SCORE, histochemistry score.

washed with PBS and incubated with 0.5% Triton X-100 for 5 min. The cells were washed with PBS and blocked with 5% goat serum at 37°C for 30 min. The cells were incubated overnight at 4°C with the primary antibody (YAP; 1:100; cat. no. 13584-1-AP, Proteintech Group, Inc.). PBST was used to wash the cells thrice, and the secondary antibody (1:200; cat. no. ab150075, Abcam) was then added followed by incubation at 37°C for 2 h. Nuclei were counterstained with DAPI (G1012, Wuhan Servicebio Technology Co., Ltd.) for 5 min at 37°C. An anti-fading solution (P0126, Beyotime Institute of Biotechnology) was added in a dropwise manner, and observation was performed with a Nikon A1+ laser confocal microscope (Nikon Corporation).

Statistical analysis. Statistical analysis was performed using SPSS 23.0 software (IBM Corp.). The statistical significance of differences between two datasets was calculated using the two-tailed paired or unpaired Student's t-test; for comparison of multiple groups, one- or two-way ANOVA was performed followed using Dunnett's for multiple post hoc comparisons. P-values <0.05 were considered to indicate statistically significant differences.

Results

The level of O-GlcNAcylation is associated with the malignancy of EC. To explore the effects of *O*-GlcNAcylation on EC, OGT and *O*-GlcNAc expression was examined in cancer tissues and paired tumor-adjacent tissues from 15 patients with EC. The results of immunohistochemistry revealed that the EC tissues expressed higher levels of OGT and *O*-GlcNAc than the paired normal tumor-adjacent endometrial tissues (Fig. 1A and B). Likewise, the OGT and *O*-GlcNAc H-SCOREs in the EC tissues were significantly higher than those in the paired tumor-adjacent tissues (Fig. 1C and D).

In addition, the association between the H-SCORE of *O*-GlcNAcylation and OGT, and the clinicopathological features of 28 patients with EC was analyzed (Tables I and II, and Fig. S1). A high staining intensity of *O*-GlcNAcylation was positive associated with lymph node metastasis, histopathological grade and clinical stage. The increased expression of OGT was positively associated with the clinical stage and lymph node metastasis, although not with the histopathological grade. Neither *O*-GlcNAcylation nor OGT expression was associated with the age of the patients.

Table I. Evaluation of the association between O-GlcNAcylation and the clinical characteristics of 28 patients with endometrial cancer.

Variable	No. of patients	H-SCORE of O-GlcNAc (± SE)	P-value
Age (years)			
<55	13	147.65±18.80	0.640505
≥55	15	150.72±15.59	
Histopathological grade			
Well differentiated	7	137.43±7.15	0.028965[a]
Moderately differentiated + poorly differentiated	21	153.25±17.45	
Clinical stage			
I + II	19	144.09±12.69	0.014766[a]
III + IV	9	160.29±20.04	
Lymph node metastasis			
Yes	8	163.81±16.87	0.002264[b]
No	20	143.49±13.30	

[a]$P<0.05$ and [b]$P<0.01$.

Table II. Evaluation of the association between OGT and the clinical characteristics of 28 patients with endometrial cancer.

Variable	No. of patients	H-SCORE of OGT (± SEM)	P-value
Age (years)			
<55	13	53.4715±24.44747	0.455603
≥55	15	47.3313±18.37585	
Histopathological grade			
Well differentiated	7	55.98±22.19	0.414238
Moderately + poorly differentiated	21	48.25±21.09	
Clinical stage			
I + II	19	38.23±20.70	0.037619[a]
III + IV	9	55.84±19.49	
Lymph node metastasis			
Yes	8	56.42±19.72	0.010983[a]
No	20	34.59±17.11	

[a]$P<0.05$. OGT, O-GlcNAc transferase.

O-GlcNAcylation is essential for the malignancy of EC cells. To examine the effects of O-GlcNAcylation on EC, the EC cells were treated with TMG and OSMI-1, which are able to regulate O-GlcNAcylation. The O-GlcNAcylation levels increase upon treatment with TMG via the antagonization of OGA activity, whereas these levels are reduced following treatment with OSMI-1 through the inhibition of OGT activity (33,34). Similar to these previous studies, the results of the present study indicated that treatment with TMG increased the O-GlcNAcylation levels, whereas treatment with OSMI-1 reduced the O-GlcNAcylation levels (Fig. 2A and B). The results of CCK-8 assay revealed that the OSMI-1-treated cells (OSMI-1 group) had a markedly impaired proliferative ability compared to the control group (DMSO group), while the TMG-treated cells (TMG group) had a significantly enhanced proliferative ability (Fig. 2C and D). In addition, the migratory ability of the aforementioned cells was examined using wound healing assays. The results revealed that the migratory ability of the cells in the OSMI-1 group was markedly reduced in comparison with the control group, while that of the TMG group was not significantly altered (Fig. 2E and F).

Subsequently, OGT-specific small hairpin RNA (shRNA) were used to construct stable OGT-deficient AN3CA and HEC-1-B cell lines. OGT expression was decreased in OGT-specific shRNA-transfected cells compared to the control (Con-sh) cells, and the O-GlcNAcylation levels were also found to be decreased (Fig. 3A and B). When compared to the control group, the OGT-deficient (OGT-sh) cells exhibited an inhibited growth capacity in the CCK-8
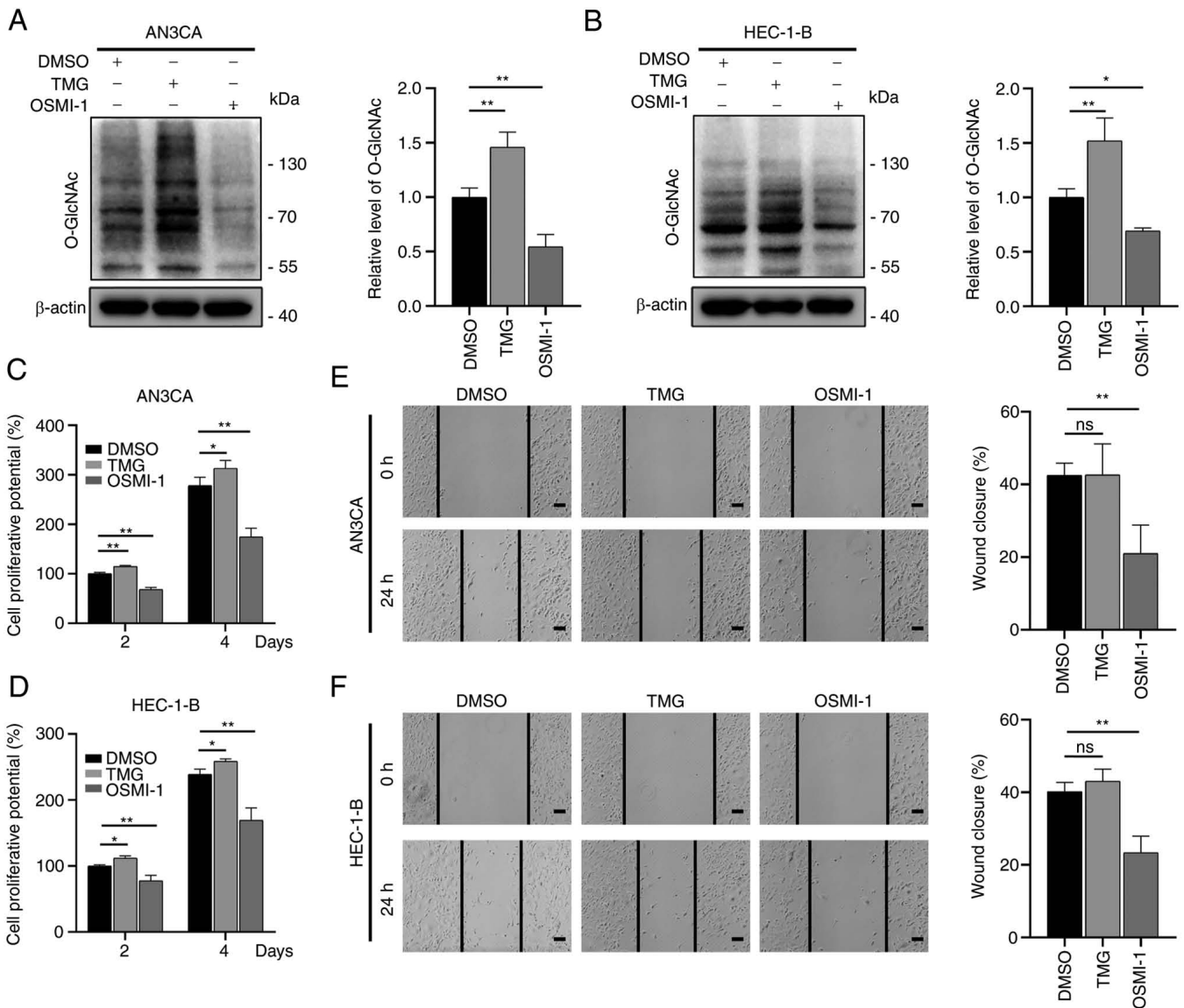
Figure 2. *O*-GlcNAcylation modulates the invasion and metastasis of endometrial cancer cells. (A and B) AN3CA and HEC-1-B cells were treated with DMSO, TMG (10 μM), or OSMI-1 (50 μM) for 24 h. Western blot analysis was used to examine *O*-GlcNAc expression. (C and D) The same number of cells was inoculated in 96-well plates with DMSO, TMG (10 μM), or OSMI (50 μM) in the medium. Cell proliferation was measured using a Cell Counting Kit-8 assay at the indicated time points. (E and F) Wound healing assays were performed to evaluate the effects of *O*-GlcNAcylation on the migratory abilities of AN3CA and HEC-1-B cells. The cells were treated with DMSO, TMG (10 μM), or OSMI-1 (50 μM). Images were obtained at 0 and 24 h after the scraping of single molecule membranes. Scale bars, 100 μm. Data represent the mean ± SD (n=3). *P<0.05 and **P<0.01. ns, not significant; TMG, Thiamet-G.

and EdU cell proliferation assays (Fig. 3C and D). The results of wound healing assay also revealed an impaired wound closure rate for the OGT-deficient cells (Fig. S2). Transwell assays were then used to assess the migratory and invasive ability of the OGT-sh group (in both AN3CA and HEC-1-B cells) and it was found that the migratory and invasive ability of the cells decreased significantly in the OGT-sh group (Fig. 3E and F). These findings demonstrate that *O*-GlcNAcylation is critical to EC proliferation and metastasis.

YAP combines with OGT and undergoes O-GlcNAcylation. In order to elucidate the mechanisms through which *O*-GlcNAcylation promotes the development of EC, the Con-sh and OGT-sh HEC-1-B cells were analyzed using high-performance liquid chromatography to identify differential proteins that could be *O*-GlcNAcylated (Fig. 4A). It was found that YAP was *O*-GlcNAcylated, and the knockdown of OGT resulted in a reduced YAP *O*-GlcNAcylation (Fig. 4A). Combined with the related genes of EC in the GeneCards database (https://www.genecards.org/) and the crucial role of YAP in EC, it was hypothesized that *O*-GlcNAcylation may affect tumor malignancy by regulating YAP. It was verified that YAP was the target protein for *O*-GlcNAcylation through co-immunoprecipitation experiments: Its *O*-GlcNAcylation level was reduced as the global *O*-GlcNAcylation decreased (Fig. 4B). Furthermore, it was demonstrated that the knockdown of YAP significantly reduced the proliferative and migratory abilities of the cells; however, altering the O-GlcNAcylation of cells following the knockdown of YAP had no significant effect on the proliferative and migratory abilities of the cells (Fig. S3).
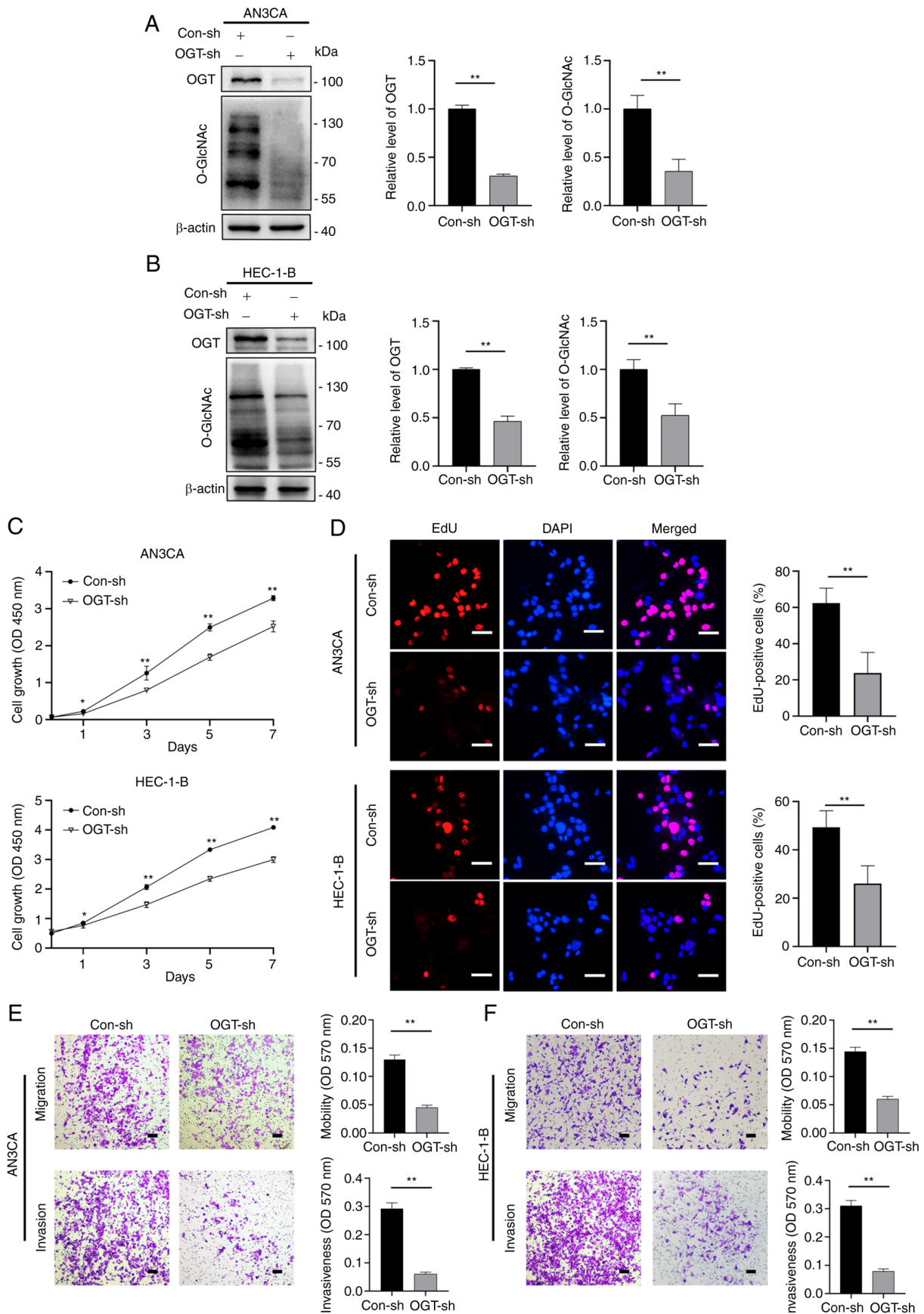
Figure 3. OGT dysregulation affects endometrial cancer cell proliferation, migration and invasion. Stable OGT-deficient cell lines and control groups were established by transfection with OGT shRNA or control. (A and B) The levels of OGT and global O-GlcNAcylation in Con-sh and OGT-sh groups of (A) AN3CA and (B) HEC-1-B cells were examined using western blot analysis. (C) Cell proliferation was measured using Cell Counting Kit-8 assays at the indicated time points. (D) EdU staining assays were used to examine the proliferative capacities of cells in the Con-sh and OGT-sh groups. Scale bars, 50 μm. (E and F) Cell migration and invasion were examined using Transwell assays. Following 48 h of culture, the Transwell membrane was stained and observed under a microscope. Scale bars, 100 μm. Data represent the mean ± SD (n=3). *P<0.05 and **P<0.01. OGT, O-GlcNAc transferase.
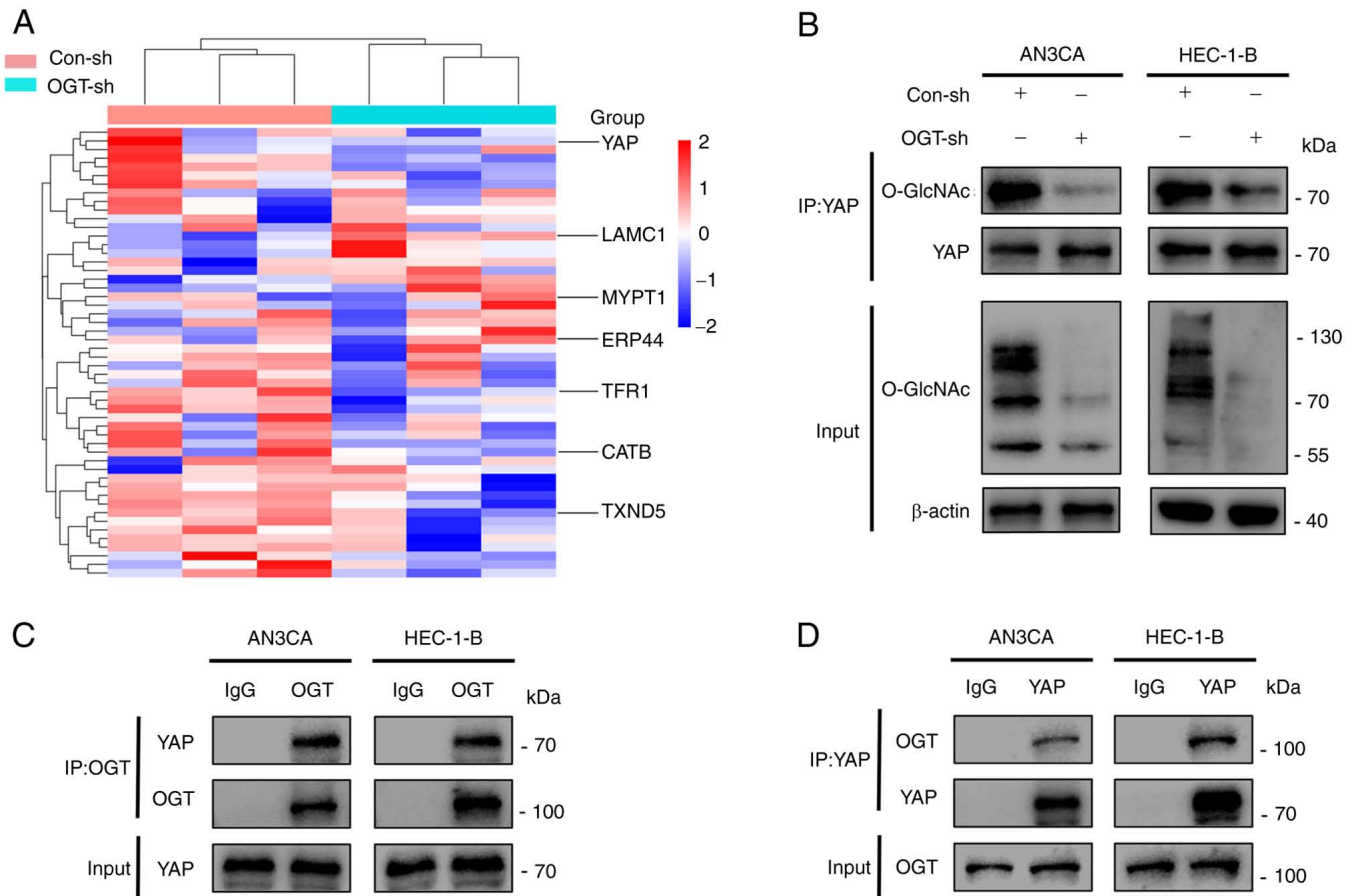
Figure 4. YAP interacts with OGT for *O*-GlcNAcylation. (A) Heatmap illustrating proteins in the Con-sh and OGT-sh groups of HEC-1-B cells that were *O*-GlcNAcylated. (B) YAP *O*-GlcNAcylation was detected using a co-immunoprecipitation assay after changing the global *O*-GlcNAcylation level. (C and D) Co-immunoprecipitation assays demonstrated the interaction between OGT and YAP in AN3CA and HEC-1-B cells. YAP, Yes-associated protein; OGT, *O*-GlcNAc transferase.

In addition, owing to the fact that OGT is the only enzyme known to promote protein *O*-GlcNAcylation, the present study examined whether YAP interacts with OGT. The result of co-immunoprecipitation assays indicated that YAP interacted with OGT (Fig. 4C and D). In summary, it was demonstrated that YAP interacts with OGT, leading to its *O*-GlcNAcylation.

YAP O-GlcNAcylation inhibits phosphorylation by suppressing YAP/LATS1/2 expression to improve the stability of YAP protein. In light of the fact that *O*-GlcNAcylation affects the expression and function of multiple proteins, the effects of *O*-GlcNAcylation on YAP expression were examined. It was observed that YAP expression was decreased in the OGT-sh group (Fig. 5A and B). YAP transcriptional levels were measured in the Con-sh and OGT-sh groups to investigate the mechanisms driving the changes in YAP expression (Fig. 5C). The transcriptional levels of YAP in the AN3CA OGT-sh group increased significantly, whereas no significant difference was found between the HEC-1-B Con-sh and OGT-sh groups (Fig. 5C). As protein concentration is regulated by synthesis and degradation, it was hypothesized that the changes in YAP expression were related to YAP degradation. As demonstrated by CHX chase experiments, OGT knockdown reduced the half-life

of YAP in EC cells (Figs. 5D and S4), indicating that O-GlcNAcylation modulates YAP expression by enhancing its stability.

Since YAP phosphorylation at Ser127 (p-YAP) inactivates YAP through cytosolic sequestration and subsequent degradation (22), it was hypothesized that the changes in YAP expression due to *O*-GlcNAcylation were associated with its phosphorylation. It was found that a decreased *O*-GlcNAcylation resulted in a significantly increased p-YAP(S127)/YAP ratio (decreased YAP expression with increased p-YAP expression; Fig. 5A and B). Through the kinase cascade reaction, YAP, a Hippo pathway effector, is phosphorylated by upstream kinases (LATS1/2) (22). Herein, to explore whether *O*-GlcNAcylation affects the phosphorylation of YAP by blocking LATS1/2 binding to YAP, co-immunoprecipitation assays were performed. The results suggested that the reduced *O*-GlcNAcylation promoted the accessibility of YAP to LATS1/2 (Fig. 5E). On the whole, the results confirmed that *O*-GlcNAcylation enhanced the stability of YAP by inhibiting its phosphorylation via the suppression of the interaction of YAP and LATS1/2.

O-GlcNAcylation of YAP regulates its activation and nuclear translocation. It has been shown that unphosphorylated YAP enters the nucleus and actives transcription factors (21).
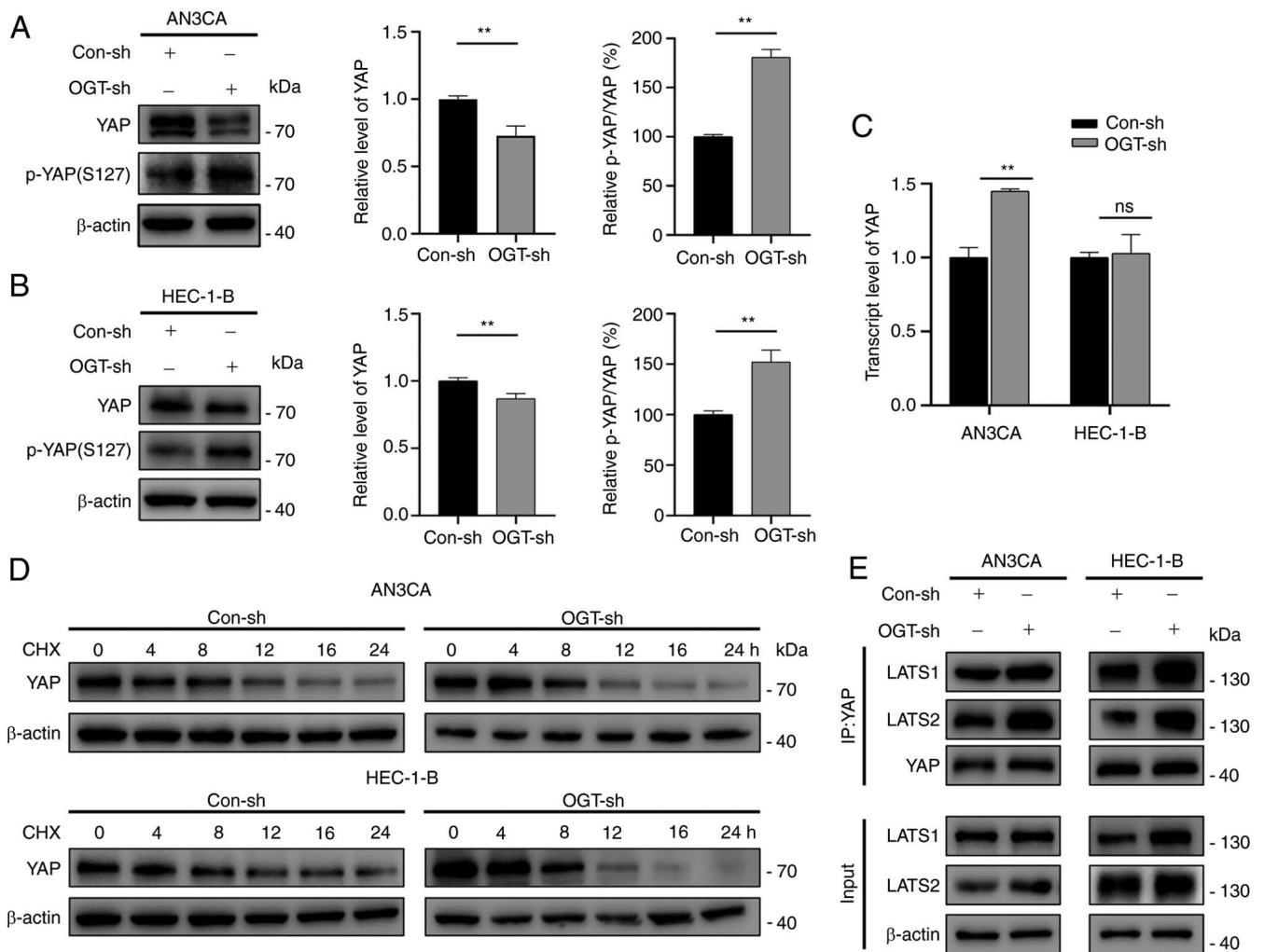
Figure 5. *O*-GlcNAcylation regulates YAP stability and phosphorylation by inhibiting the YAP/LATS1/2 interaction. (A and B) Western blot analysis of YAP and p-YAP expression levels in the Con-sh and OGT-sh groups of (A) AN3CA and (B) HEC-1-B cells. (C) mRNA expression levels of YAP in the Con-sh and OGT-sh groups of endometrial cancer cells. (D) CHX chase experiments were used to measure YAP expression at different time points following treatment of the cells with CHX (50 μM). (E) Co-immunoprecipitation assay revealed that *O*-GlcNAcylation affected the YAP-LATS1/2 interaction. Data represent the mean ± SD (n=3). **P<0.01. ns, not significant; YAP, Yes-associated protein; OGT, *O*-GlcNAc transferase; CHX, cycloheximide.

However, whether YAP *O*-GlcNAcylation leads to induces YAP nuclear entry remains unclear. Therefore, the present study examined the distribution of YAP by separating nuclear and cytoplasmic proteins. It was observed that YAP expression was markedly reduced in the nucleus and slightly decreased in the cytoplasm of the OGT-sh group (Fig. 6A). These results were in accordance with those obtained by immunofluorescence staining, which confirmed that YAP in the OGT-sh group was predominantly located in the cytoplasm and less in the nucleus compared to the control group (Fig. 6B and C).

Further research was conducted on the mRNA expression of typical YAP target genes (ANKRD1, CTGF, CYR61 and GLUT3) to examine the effects of *O*-GlcNAcylation on YAP activity (Fig. 6D and E). The results revealed that a decrease in *O*-GlcNAcylation reduced the transcriptional levels of YAP downstream target genes (Fig. 6D and E). Subsequently, the protein expression of CTGF was verified using western blot analysis. Consistent with the results obtained for mRNA expression, reduced *O*-GlcNAcylation resulted in a decreased expression of CTGF (Fig. 6F). Thus, these results demonstrate

that YAP nuclear distribution and activation are influenced by its *O*-GlcNAcylation level.

Discussion

By comparing EC tissues with normal tumor-adjacent endometrial tissues, the present study found that OGT and *O*-GlcNAcylation were significantly upregulated in EC tissues. *O*-GlcNAcylation was positively associated with lymph node metastasis, histopathological grade and clinical stage, while OGT expression was positively associated with clinical stage and lymph node metastasis, although not with histopathological grade. *O*-GlcNAcylation in tissues may not only be regulated via OGT, but also by OGA and the nutritional status *in vivo*; however, the sample size in the present study was not sufficient to cover all these aspects. In subsequent experiments, it was confirmed that the reduction of *O*-GlcNAcylation affected EC cell proliferation, migration and invasion.

In EC cells and tissues, YAP is upregulated and its expression is significantly associated with tumor grade,
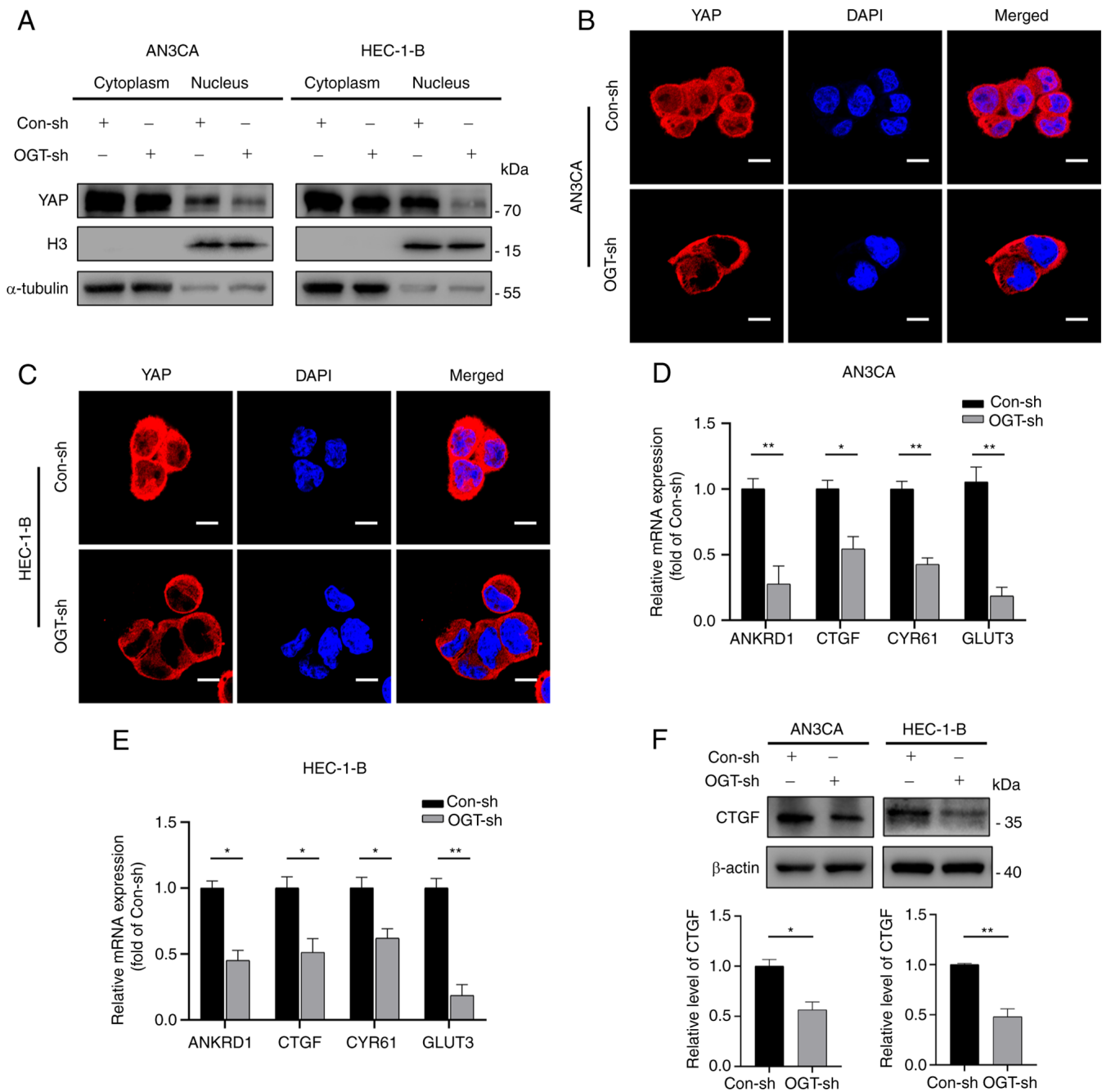
Figure 6. YAP *O*-GlcNAcylation promotes its activation and nuclear translocation. (A) Nuclear-cytoplasmic separation assays revealed the cellular sub-localization of YAP in the different groups. (B and C) Immunofluorescence staining revealed the cellular sub-localization of YAP in the different groups. Scale bars, 10 μm. (D and E) mRNA expression of ANKRD1, CTGF, CYR61 and GLUT3 was detected in endometrial cancer using reverse transcription-quantitative PCR in EC cells. (F) Western blot analysis was used to measure CTGF expression in endometrial cancer cells. Data represent the mean ± SD (n=3). *P<0.05 and **P<0.01. ns, not significant; YAP, Yes-associated protein; OGT, *O*-GlcNAc transferase; H3, Histone-H3; ANKRD1, ankyrin repeat domain 1; CTGF, connective tissue growth factor; CYR61, cysteine-rich angiogenic inducer 61; GLUT3, glucose transporter 3.

stage, post-operative recurrence/metastasis, and overall survival (35-37). As YAP expression and function are controlled by its phosphorylation (38), altering its phosphorylation affects the malignancy of a variety of tumors by influencing YAP activation and nucleation (39,40). YAP *O*-GlcNAcylation hinders its phosphorylation, thus facilitating YAP entry into the nucleus to exert pro-cancer effects (41,42). Based on these findings, the present study identified that YAP was *O*-GlcNAcylated in EC cells and that this modification affected its expression. Further analyses revealed

that a reduction in the global *O*-GlcNAcylation levels in EC cells resulted in the decreased *O*-GlcNAcylation of YAP and promoted YAP phosphorylation by facilitating the binding of YAP to LATS1/2, leading to its cytoplasmic retention and functional inactivation.

It has been demonstrated that downstream target genes of YAP play a crucial role in tumorigenesis. CTGF is a multifunctional signaling regulator that promotes cancer development, progression and metastasis by regulating cell proliferation (43). CTGF has been found to be an independent
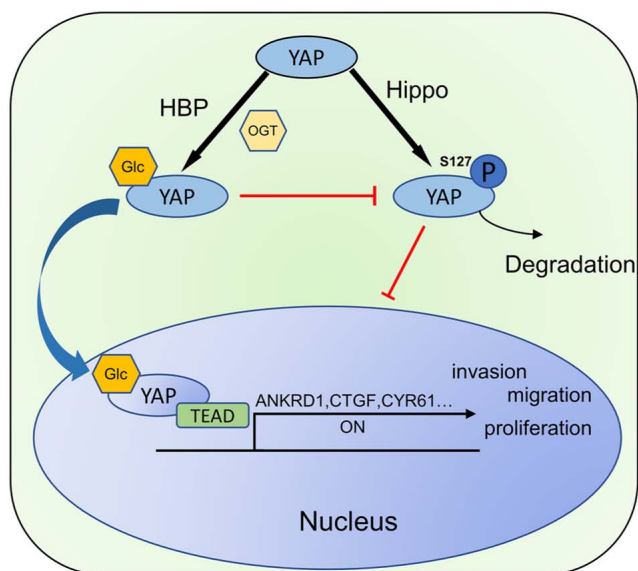
Figure 7. Schematic diagram illustrating that *O*-GlcNAcylation affects the malignancy of endometrial cancer by regulating the activity and phosphorylation of YAP. YAP, Yes-associated protein; OGT, *O*-GlcNAc transferase; ANKRD1, ankyrin repeat domain 1; CTGF, connective tissue growth factor; CYR61, cysteine-rich angiogenic inducer 61; HBP, hexosamine-biosynthesis pathway; Glc, glucose; TEAD, TEA domain transcription factor; ON, downstream pathway activation.

prognostic factor in EC; it is closely associated with the development of EC and can be used as a prognostic biomarker in EC (44). GLUT3 is a member of the GLUT family and is involved in the first step of cellular glucose utilization and glycolysis. It has been found that GLUT3 is involved in glucose uptake by EC cells and is associated with the degree of differentiation of EC (45). CYR61 is a dynamically expressed multifunctional matricellular protein that is associated with the proliferative capacity of EC cells (46). A key mechanism through which YAP exerts its influence on tumor function is by regulating the expression of its downstream target proteins (47). YAP promotes the proliferation and migration of colorectal cancer cells through the GLUT3/AMPK signaling pathway (48); the Hippo-YAP pathway upregulates CYR61/CTGF to promote the aggressive phenotype of thyroid cancer (49). The authors aim to focus on exploring the function of downstream target genes of YAP protein in EC and to further explore the localization of YAP and its downstream target genes in EC tissue in future studies.

There is a frequent and dynamic crosstalk between *O*-GlcNAcylation and phosphorylation. These PTMs can compete for the same sites/residues (50,51) and occur on Ser/Thr residues both at close distances from one another (52,53) and relatively far from one another (54). This crosstalk is reflected in YAP by the fact that *O*-GlcNAcylation and phosphorylation occur at residues in close proximity and that the PTMs have specific effects on the function of the protein. When YAP is *O*-GlcNAcylated at threonine 241, its serine 127 phosphorylation is inhibited, which promotes YAP nuclear translocation in hepatocellular carcinoma cells (41). YAP undergoes *O*-GlcNAcylation at serine 109, competing with serine 127 phosphorylation (42,55). The present study identified the *O*-GlcNAcylation site of YAP

in EC cells by mass spectrometry (Fig. S5); however, the present study only demonstrated that the *O*-GlcNAcylation of YAP hinders the phosphorylation of serine 127. The specific PTM site that affects YAP phosphorylation needs further investigation.

In conclusion, the present study demonstrated elevated *O*-GlcNAcylation levels in EC and explored the mechanisms of the tumorigenic role of *O*-GlcNAcylation. It was demonstrated for the first time, to the best of our knowledge, that the *O*-GlcNAcylation of YAP affects the phosphorylation of its serine 127 site, which in turn regulates the malignancy of EC (Fig. 7). The results obtained herein suggest that targeting YAP *O*-GlcNAcylation may represent a promising therapeutic strategy for EC.

Availability of data and materials

The datasets used and/or analyzed during the current study are available from the corresponding author upon reasonable request. The data obtained from mass spectrometric analysis are available at: https://www.iprox.cn/page/PSV023. html;?url=1685362579736KfYS (password: HJVv).

Authors' contributions

FZ and BC designed the study. LZ and XY were involved in the conceptualization of the study. LZ, JD and LQ performed the experiments. YG, YL and LC were involved in data processing. LZ, FZ and XY confirm the authenticity of all the raw data. LZ, XY and FZ were involved in the writing of the manuscript. FZ and BC supervised the study. All the authors were involved in the discussions related to the manuscript. All authors have read and approved the final manuscript.

Ethics approval and consent to participate

Ethics approval (no. KY20203047) was provided by the Medical Ethics Committee of the First Hospital Affiliated to the Air Force Medical University (Xi'an, China).

Patient consent for publication

Not applicable.

Competing interests

The authors declare that they have no competing interests.

References

1. Siegel RL, Miller KD, Fuchs HE and Jemal A: Cancer statistics, 2021. CA Cancer J Clin 71: 7-33, 2021.
2. Urick ME and Bell DW: Clinical actionability of molecular targets in endometrial cancer. Nat Rev Cancer 19: 510-521, 2019.
3. Brooks RA, Fleming GF, Lastra RR, Lee NK, Moroney JW, Son CH, Tatebe K and Veneris JL: Current recommendations and recent progress in endometrial cancer. CA Cancer J Clin 69: 258-279, 2019.
4. Shahid RK, Ahmed S, Le D and Yadav S: Diabetes and cancer: Risk, challenges, management and outcomes. Cancers (Basel) 13: 5735, 2021.
5. Lam C, Low JY, Tran PT and Wang H: The hexosamine biosynthetic pathway and cancer: Current knowledge and future therapeutic strategies. Cancer Lett 503: 11-18, 2021.
6. Ma J, Wu C and Hart GW: Analytical and biochemical perspectives of protein O-GlcNAcylation. Chem Rev 121: 1513-1581, 2021.
7. Yang X and Qian K: Protein O-GlcNAcylation: Emerging mechanisms and functions. Nat Rev Mol Cell Biol 18: 452-465, 2017.
8. Chang YH, Weng CL and Lin KI: O-GlcNAcylation and its role in the immune system. J Biomed Sci 27: 57, 2020.
9. Akimoto Y, Yan K, Miura Y, Tsumoto H, Toda T, Fukutomi T, Sugahara D, Kudo A, Arai T, Chiba Y, *et al*: O-GlcNAcylation and phosphorylation of β-actin Ser199 in diabetic nephropathy. Am J Physiol Renal Physiol 317: F1359-F1374, 2019.
10. Nie H and Yi W: O-GlcNAcylation, a sweet link to the pathology of diseases. J Zhejiang Univ Sci B 20: 437-448, 2019.
11. Lee BE, Suh PG and Kim JI: O-GlcNAcylation in health and neurodegenerative diseases. Exp Mol Med 53: 1674-1682, 2021.
12. Quik M, Hokke CH and Everts B: The role of O-GlcNAcylation in immunity against infections. Immunology 161: 175-185, 2020.
13. Lee JB, Pyo KH and Kim HR: Role and function of O-GlcNAcylation in cancer. Cancers (Basel) 13: 5365, 2021.
14. Ferrer CM, Lynch TP, Sodi VL, Falcone JN, Schwab LP, Peacock DL, Vocadlo DJ, Seagroves TN and Reginato MJ: O-GlcNAcylation regulates cancer metabolism and survival stress signaling via regulation of the HIF-1 pathway. Mol Cell 54: 820-831, 2014.
15. Sun L, Lv S and Song T: O-GlcNAcylation links oncogenic signals and cancer epigenetics. Discov Oncol 12: 54, 2021.
16. Jaskiewicz NM and Townson DH: Hyper-O-GlcNAcylation promotes epithelial-mesenchymal transition in endometrial cancer cells. Oncotarget 10: 2899-2910, 2019.
17. Ciesielski P, Jóźwiak P, Forma E and Krześlak A: TET3- and OGT-dependent expression of genes involved in epithelial-mesenchymal transition in endometrial cancer. Int J Mol Sci 22: 13239, 2021.
18. Ma S, Meng Z, Chen R and Guan KL: The Hippo pathway: Biology and pathophysiology. Annu Rev Biochem 88: 577-604, 2019.
19. Wang S, Zhou L, Ling L, Meng X, Chu F, Zhang S and Zhou F: The crosstalk between Hippo-YAP pathway and innate immunity. Front Immunol 11: 323, 2020.
20. Ibar C and Irvine KD: Integration of Hippo-YAP signaling with metabolism. Dev Cell 54: 256-267, 2020.
21. Piccolo S, Dupont S and Cordenonsi M: The biology of YAP/TAZ: Hippo signaling and beyond. Physiol Rev 94: 1287-1312, 2014.
22. Misra JR and Irvine KD: The Hippo signaling network and its biological functions. Annu Rev Genet 52: 65-87, 2018.
23. Dey A, Varelas X and Guan KL: Targeting the Hippo pathway in cancer, fibrosis, wound healing and regenerative medicine. Nat Rev Drug Discov 19: 480-494, 2020.
24. Chao ML, Luo S, Zhang C, Zhou X, Zhou M, Wang J, Kong C, Chen J, Lin Z, Tang X, *et al*: S-nitrosylation-mediated coupling of G-protein alpha-2 with CXCR5 induces Hippo/YAP-dependent diabetes-accelerated atherosclerosis. Nat Commun 12: 4452, 2021.
25. Wei F, Wang A, Wang Q, Han W, Rong R, Wang L, Liu S, Zhang Y, Dong C and Li Y: Plasma endothelial cells-derived extracellular vesicles promote wound healing in diabetes through YAP and the PI3K/Akt/mTOR pathway. Aging (Albany NY) 12: 12002-12018, 2020.
26. Ortillon J, Le Bail JC, Villard E, Léger B, Poirier B, Girardot C, Beeske S, Ledein L, Blanchard V, Brieu P, *et al*: High glucose activates YAP signaling to promote vascular inflammation. Front Physiol 12: 665994, 2021.
27. Zanconato F, Cordenonsi M and Piccolo S: YAP/TAZ at the roots of cancer. Cancer Cell 29: 783-803, 2016.
28. Nguyen CDK and Yi C: YAP/TAZ signaling and resistance to cancer therapy. Trends Cancer 5: 283-296, 2019.
29. Konno T, Kohno T, Okada T, Shimada H, Satohisa S, Kikuchi S, Saito T and Kojima T: ASPP2 suppression promotes malignancy via LSR and YAP in human endometrial cancer. Histochem Cell Biol 154: 197-213, 2020.
30. Zhu G, Murshed A, Li H, Ma J, Zhen N, Ding M, Zhu J, Mao S, Tang X, Liu L, *et al*: O-GlcNAcylation enhances sensitivity to RSL3-induced ferroptosis via the YAP/TFRC pathway in liver cancer. Cell Death Discov 7: 83, 2021.
31. Safran M, Dalah I, Alexander J, Rosen N, Iny Stein T, Shmoish M, Nativ N, Bahir I, Doniger T, Krug H, *et al*: GeneCards version 3: The human gene integrator. Database (Oxford) 2010: baq020, 2010.
32. Livak KJ and Schmittgen TD: Analysis of relative gene expression data using real-time quantitative PCR and the 2(-Delta Delta C(T)) method. Methods 25: 402-408, 2001.
33. Wu J, Tan Z, Li H, Lin M, Jiang Y, Liang L, Ma Q, Gou J, Ning L, Li X and Guan F: Melatonin reduces proliferation and promotes apoptosis of bladder cancer cells by suppressing O-GlcNAcylation of cyclin-dependent-like kinase 5. J Pineal Res 71: e12765, 2021.
34. Takeuchi T, Horimoto Y, Oyama M, Nakatani S, Kobata K, Tamura M, Arata Y and Hatanaka T: Osteoclast differentiation is suppressed by increased O-GlcNAcylation due to thiamet G treatment. Biol Pharm Bull 43: 1501-1505, 2020.
35. Wang J, Song T, Zhou S and Kong X: YAP promotes the malignancy of endometrial cancer cells via regulation of IL-6 and IL-11. Mol Med 25: 32, 2019.
36. Tsujiura M, Mazack V, Sudol M, Kaspar HG, Nash J, Carey DJ and Gogoi R: Yes-associated protein (YAP) modulates oncogenic features and radiation sensitivity in endometrial cancer. PLoS One 9: e100974, 2014.
37. Cheng Y, Huang H, Han Y and Zhu Y: Expression of YAP in endometrial carcinoma tissues and its effect on epithelial to mesenchymal transition. Transl Cancer Res 9: 7248-7258, 2020.
38. Yan F, Qian M, He Q, Zhu H and Yang B: The posttranslational modifications of Hippo-YAP pathway in cancer. Biochim Biophys Acta Gen Subj 1864: 129397, 2020.
39. Ni W, Yao S, Zhou Y, Liu Y, Huang P, Zhou A, Liu J, Che L and Li J: Long noncoding RNA GAS5 inhibits progression of colorectal cancer by interacting with and triggering YAP phosphorylation and degradation and is negatively regulated by the m6A reader YTHDF3. Mol Cancer 18: 143, 2019.
40. Wang R, Du Y, Shang J, Dang X and Niu G: PTPN14 acts as a candidate tumor suppressor in prostate cancer and inhibits cell proliferation and invasion through modulating LATS1/YAP signaling. Mol Cell Probes 53: 101642, 2020.
41. Zhang X, Qiao Y, Wu Q, Chen Y, Zou S, Liu X, Zhu G, Zhao Y, Chen Y, Yu Y, *et al*: The essential role of YAP O-GlcNAcylation in high-glucose-stimulated liver tumorigenesis. Nat Commun 8: 15280, 2017.
42. Peng C, Zhu Y, Zhang W, Liao Q, Chen Y, Zhao X, Guo Q, Shen P, Zhen B, Qian X, *et al*: Regulation of the Hippo-YAP pathway by glucose sensor O-GlcNAcylation. Mol Cell 68: 591-604 e5, 2017.
43. Shen YW, Zhou YD, Chen HZ, Luan X and Zhang WD: Targeting CTGF in cancer: An emerging therapeutic opportunity. Trends Cancer 7: 511-524, 2021.
44. Li XT, Li JY, Zeng GC, Lu L, Jarrett MJ, Zhao Y, Yao QZ, Chen X and Yu KJ: Overexpression of connective tissue growth factor is associated with tumor progression and unfavorable prognosis in endometrial cancer. Cancer Biomark 25: 295-302, 2019.
45. Krzeslak A, Wojcik-Krowiranda K, Forma E, Jozwiak P, Romanowicz H, Bienkiewicz A and Brys M: Expression of GLUT1 and GLUT3 glucose transporters in endometrial and breast cancers. Pathol Oncol Res 18: 721-728, 2012.
46. MacLaughlan SD, Palomino WA, Mo B, Lewis TD, Lininger RA and Lessey BA: Endometrial expression of Cyr61: A marker of estrogenic activity in normal and abnormal endometrium. Obstet Gynecol 110: 146-154, 2007.
47. Kim H, Son S, Ko Y, Lee JE, Kim S and Shin I: YAP, CTGF and Cyr61 are overexpressed in tamoxifen-resistant breast cancer and induce transcriptional repression of ERα. J Cell Sci 134: jcs256503, 2021.
48. Kuo CC, Ling HH, Chiang MC, Chung CH, Lee WY, Chu CY, Wu YC, Chen CH, Lai YW, Tsai IL, *et al*: Metastatic colorectal cancer rewrites metabolic program through a Glut3-YAP-dependent signaling circuit. Theranostics 9: 2526-2540, 2019.
49. Kuo CY, Chang YC, Chien MN, Jhuang JY, Hsu YC, Huang SY and Cheng SP: SREBP1 promotes invasive phenotypes by upregulating CYR61/CTGF via the Hippo-YAP pathway. Endocr Relat Cancer 29: 47-58, 2021.

50. Cheng X and Hart GW: Alternative O-glycosylation/ O-phosphorylation of serine-16 in murine estrogen receptor beta: Post-translational regulation of turnover and transactivation activity. J Biol Chem 276: 10570-10575, 2001.
51. Hardivillé S, Hoedt E, Mariller C, Benaïssa M and Pierce A: O-GlcNAcylation/phosphorylation cycling at Ser10 controls both transcriptional activity and stability of delta-lactoferrin. J Biol Chem 285: 19205-19218, 2010.
52. Rani L, Mittal J and Mallajosyula SS: Effect of phosphorylation and O-GlcNAcylation on proline-rich domains of tau. J Phys Chem B 124: 1909-1918, 2020.
53. Fu Y, Ning L, Feng J, Yu X, Guan F and Li X: Dynamic regulation of O-GlcNAcylation and phosphorylation on STAT3 under hypoxia-induced EMT. Cell Signal 93: 110277, 2022.
54. Whelan SA, Lane MD and Hart GW: Regulation of the O-linked beta-N-acetylglucosamine transferase by insulin signaling. J Biol Chem 283: 21411-21417, 2008.
55. Li X, Wu Z, He J, Jin Y, Chu C, Cao Y, Gu F, Wang H, Hou C, Liu X and Zou Q: OGT regulated O-GlcNAcylation promotes papillary thyroid cancer malignancy via activating YAP. Oncogene 40: 4859-4871, 2021.